Robotica (2000) volume 18, pp. 43–49. Printed in the United Kingdom © 2000 Cambridge University Press

Slip phase isolating: impulsive signal generating vibrotactile sensor and its application to real-time object regrip control

Yoji Yamada,* Hiroyuki Morita** and Yoji Umetani*

SUMMARY

This paper mainly concerns a vibrotactile sensor capable of generating impulsive high-frequency signals for exclusively distinguishing a slip phase from various other contact phases. We describe the structure of the vibrotactile sensor with surface ridges and, after analyzing the slip signals, conclude that the output signal originates in the free vibration of the ridge. By using a two-fingered robot hand with the sensor attached to its compliant endtips, we verify that the vibrotactile sensor has a slip phase isolating function and demonstrate object regrip control in real time.

KEYWORDS: Vibrotactile sensor; Impulsive signal; Slip phase; Two-fingered hand.

1. INTRODUCTION

1.1. Background

Early in the 1970s, Ueda *et al*. made the first proposal of slip detection sensors[1] for material handling operations of industrial robots. Since then, various types of vibrotactile sensors have been reported. Slip detection is indispensable not only to assuring the firm grasp of an object,[2] as well as to detecting its static friction coefficient.[3,4]

The subject which has been considered to be most appropriate for studying slip detection on a compliant surface of a robot finger is stick-slip vibration from the viewpoint of tribology.[5] However, a major problem arises in picking up the signals which distinctively convey slip information during manipulation tasks. This is because the frequency of the stick-slip signal is so close to those generated by other events such as impacts, grasping contacts, sliding across a surface, and noise that it is difficult to distinguish a slip phase from other contact phases. Eberman *et al*. addressed this problem and proposed techniques of segmenting and labeling each of the above events based on a generalized sequential likelihood ratio test.[6] Son *et al*. also identified the above problem and proposed a method of applying a multi-element stess rate sensor array to detecting three parameters; contact events, local skin curvature, and incipient slip.[7] Much has been gained from these contributions; especially, the slip prediction using incipient slip information which was originally proposed by Tremblay *et al*.,[8] is a promising approach to real-time grasp force control of a robot hand. However, problems still remained in that (1) such slip sensor signals do not clearly identify slipping contact phases and have a tendency to mistake them for rolling phases, and (2) the slip signals may not always be used reliably for grasping force control after they detect the complete slip of an object in practical applications.

* Toyota Technological Institute, 2-12-1, Hisakata, Tempaku, Nagoya 468-8511 (Japan)
E-mail: yamada@toyota-ti.ac.jp
** Denso Co. Ltd., 1-1 Showa-cho, Kariya 448-0029 (Japan)

1.2. Slip vibration

To resolve the above problems, we considered it desirable that a vibrotactile sensor be capable of generating characteristic slip signals of much higher frequency in the order of several to ten kiloherz: it was reported that two kinds of principal vibration phenomena can be observed when rubber slips against a steel slider in a razor blade shape; stick-slip vibration and microvibration of higher frequency.[9] High-frequency microvibration is dependent only on the skin material and the shape of the body in vibration, and is independent of other surface states while stick-slip vibration largely depends upon the normal components of contact force, the static friction coefficient, the surface profile, and other factors. Microvibration is considered to originate in free vibration when the compliant skin surface is released from constraint. By taking full advantage of the characteristic microvibration of higher frequency, we set out to examine the signal even in a complete slip phase and use that slip information to readjust the grasp force of a robot hand in real time.

1.3. Contents of the paper

In the paper, we propose a vibrotactile sensor[10] capable of generating impulsive high-frequency slip signals. After describing the structure and the circuit of the sensor, we observe the component of the sensor output indicating slip and find that it corresponds to the sensor signal detected when a surface ridge locally oscillates in a free vibration mode at the time an object is slipping on the sensor surface. We then analyze the sensor signal originating in an object in a slip phase and conclude that the signal has two kinds of significant components: one is generated by stick-slip vibration, and the other by free vibration. Furthermore, we show through the experiments using two robot fingers which enable them to grasp and simply manipulate an object, that we can isolate, *i.e.* exclusively distinguish, a slip phase of the object from other contact phases, which is a topic that has not been rigorously studied so far. Finally, we demonstrate that the slip prediction approach to prevent an object from falling using incipient slip information does not necessarily function effectively for flat sensor surfaces, and that the sensor output signal which exclusively identifies the

https://doi.org/10.1017/S0263574799002453 Published online by Cambridge University Press

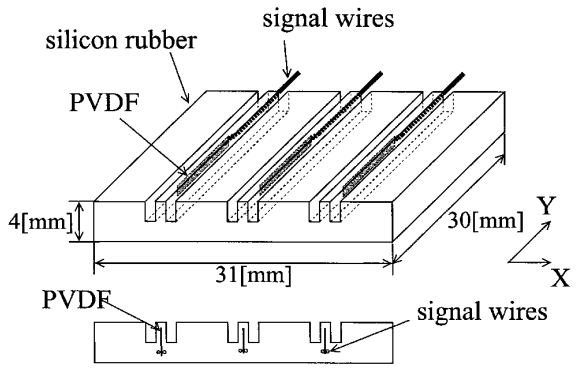


Fig. 1. Structure of the proposed vibrotactile sensor with surface ridges.

slip of an object is capable of instructing the two robot fingers to increase their grasp force.

2. VIBROTACTILE SENSOR

Figure 1 shows the structure of the sensor with surface ridges. The sensor detects slip in the X direction. A molding process was used to produce microgrooves aligned in the Y direction in the silicon rubber surface of the sensor with Young's Modulus and Poisson's ratio of the silicon rubber being $1.8\times10^3 MP_a$ and 0.95 respectively. The cross-sectional size of the sensor element whose main component is a PVDF film transducer[11,12] (KF Piezofilm, Kureha Chemical Industry Co. Ltd.) is $1\ mm\times1.5\ mm$, while that of the plane surface between the two elements is $5\ mm\times1.5\ mm$. The width of the microgroves gap is $1.5\ mm$. The PVDF film strips which measure $10\ mm\times2\ mm$ are vertically sandwiched in the center of the ridges (between the grooves). Signal wires are bonded to each side of the film using an electroconductive. The two signal wires on each ridge are connected through shielded cables to a differential amplifier circuit (AD847, ANALOG DEVICES Co. Ltd.) which is used to reject the common mode noise superposed on the PVDF film strips and/or signal lines.

3. EXPERIMENT FOR ANALYZING THE SLIP SIGNALS

We conducted the first experiment to determine whether the waveforms of the slip signals have characteristics that are distinctive enough to allow identification. Figure 2 illustrates the test apparatus for analyzing the slip signals. Its main components are a rigid frame supporting the sensor

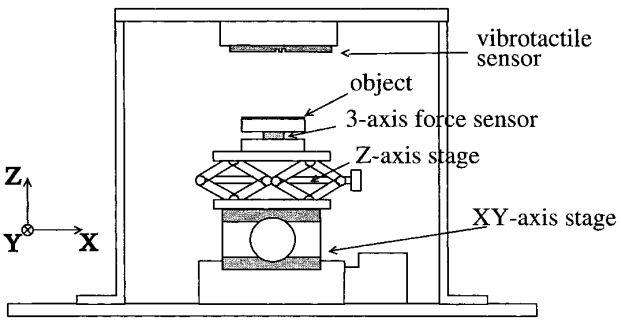


Fig. 2. Test apparatus for analyzing the slip signals.

and an XY-axis stage for moving an object linearly in the X and Y directions. A Z-axis stage is set on the XY-axis stage to manually adjust the height of the object to assure good contact between the sensor and the object. Moreover, a 3-axis force sensor is mounted just below the object to measure the normal component of the contact force.

3.1. Experimental results for generating slip signals

First of all, the static friction coefficient of a sensor surface with ridges was compared with one without ridges, and the difference was 0.02 which was 5% of the coefficient. We considered that robot hands equipped with sensors with microgrooved surfaces did not have a significant disadvantage in grasping/manipulating an object.

Figure 3 shows sample slip signals of the vibrotactile sensor output when an object, either an aluminum plate, a plastic plate, or a paper sheet, was slid on the sensor surface. In the experiment, an object was slid at 16 *mm/s* in the X direction, and the normal pressure was kept at 7.5×10^{-4} N/mm^2. Figure 3a shows the slip signals when the object was an aluminum plate, Figure 3b a plastic plate, and Figure 3c a paper sheet. In each case, the sensor output generated impulsive high-frequency signals. However, the sensor did not generate any significant signal in a stick phase. Note that the impulse duration is in the order of sub-milliseconds.

Moreover, the amplitude of the impulsive slip signals in Figures 3 was not always the same. We consider that this is

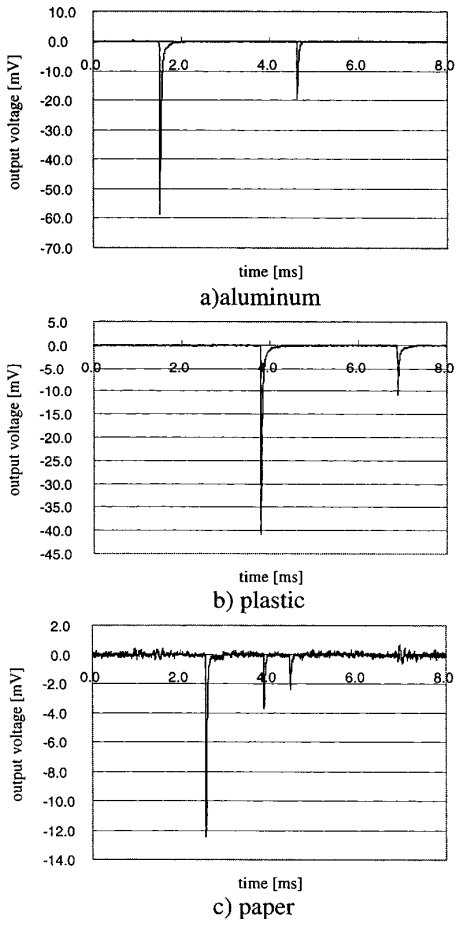


Fig. 3. Sample slip signals of the sensor output when an aluminum plate, a plastic plate, or a paper sheet is slid on the sensor surface.

https://doi.org/10.1017/S0263574799002453 Published online by Cambridge University Press

because the condition of the object surface was not consistent throughout the experiment. Taking into account of the mechanism of stick-slip vibration phenomena, we expected that a longer stick period would result in a larger sensor output amplitude, because the output was generated during the release stage of the sensor element.

For example, Figure 3 shows a slip phase at the time of the first impulsive signal and this reverts to a stick phase until the second slip signal is generated. The amount of bending strain at the ridge in a stick phase when it is bent in a tangential (X) direction is assumed to be proportional to the amplitude of the next impulsive output signal which is generated when the ridge is released again. Because the speed of the X-axis stage was kept constant in our experiment, the stick duration and the amount of strain in the stick phase are also proportional to each other. Therefore, we conclude that the stick duration is proportional to the amplitude of the impulsive slip signal. Figures 4a through c show the correlation between the amplitude of the impulsive slip signals and the stick duration. The coefficient of determination for each regression is calculated as R^2 in the lower left corner of each figure. The regression results prove the above assumption of proportionality. Consequently, the frequency of stick-slip vibration was proved to be dependent on the contact surface condition.

3.2. Wavelet analysis of the slip signals showing their correspondence with the signal in a free vibration mode

If we assume that the sensor output in the slip phase is due to free vibration of the ridge, we can say that the signals in the two cases exhibit a high degree of coherence in both free vibration mode of the ridge and the slip phase of the contact surface. Thus, we analyze the sensor output signals by applying a discrete wavelet transform and discuss the coherence in time-frequency parametric space because the slip signals are not periodic. We therefore concluded that applying simple frequency analysis would not be appropriate for our objective. We adopted a Symlet ($N = 8$) base function. The graphs in Figure 5 show the result of wavelet analysis for a: slip signal in a free vibration mode (free vibration of the sensor ridge was attained by simply plucking it). b: Slip signal on the aluminum plate, c: slip signal on the plastic plate, and d: slip signal on the paper sheet respectively. The top in each figure shows the original slip signal of the sensor output to be wavelet transformed, and the remaining three graphs represent wavelet coefficients $d1$, $d2$, and $d3$ respectively.

When comparison is made between a and {b, c and d} in view of the waveform of each wavelet coefficient, the period in which the frequency component exists for each of the coefficients appear similar, although in each graph the amplitude is different because it naturally depends on that of the original output signal. The d1 and d2 in Figure 5b show a major difference from those in Figure 5a, 5c and 5d. This discrepancy results from both a slight dull at the rising edge and the little thicker shape in the settling period after the peak which are observed in the output waveform in Figure 5b. However, the $d3$ waveform patterns which represent the main lobe of the output waveform are considered to be the same in all cases.

From the analysis, we can be fairly certain that the slip signals generated in slip phases originate in free vibration of

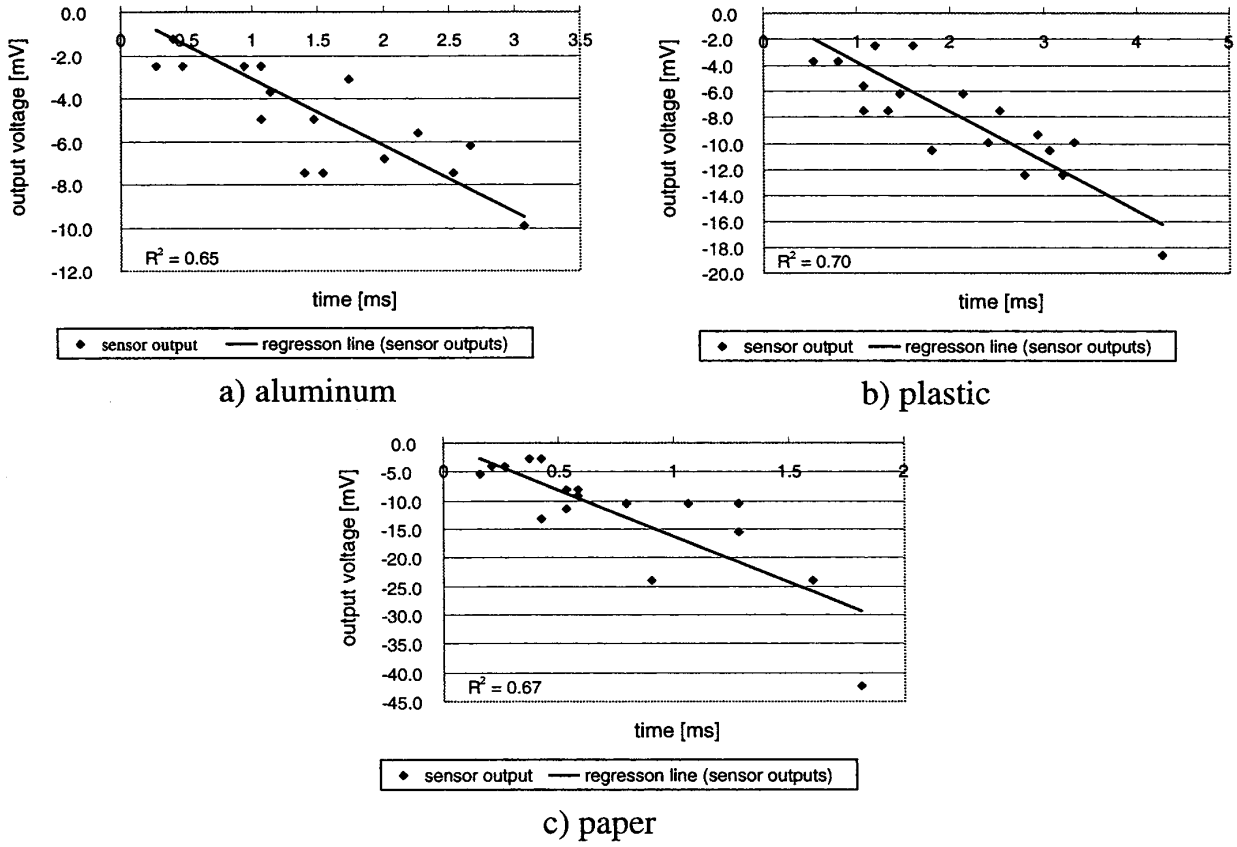


Fig. 4. Correlation between the sensor outputs and the stick duration for the three kinds of objects.

https://doi.org/10.1017/S0263574799002453 Published online by Cambridge University Press

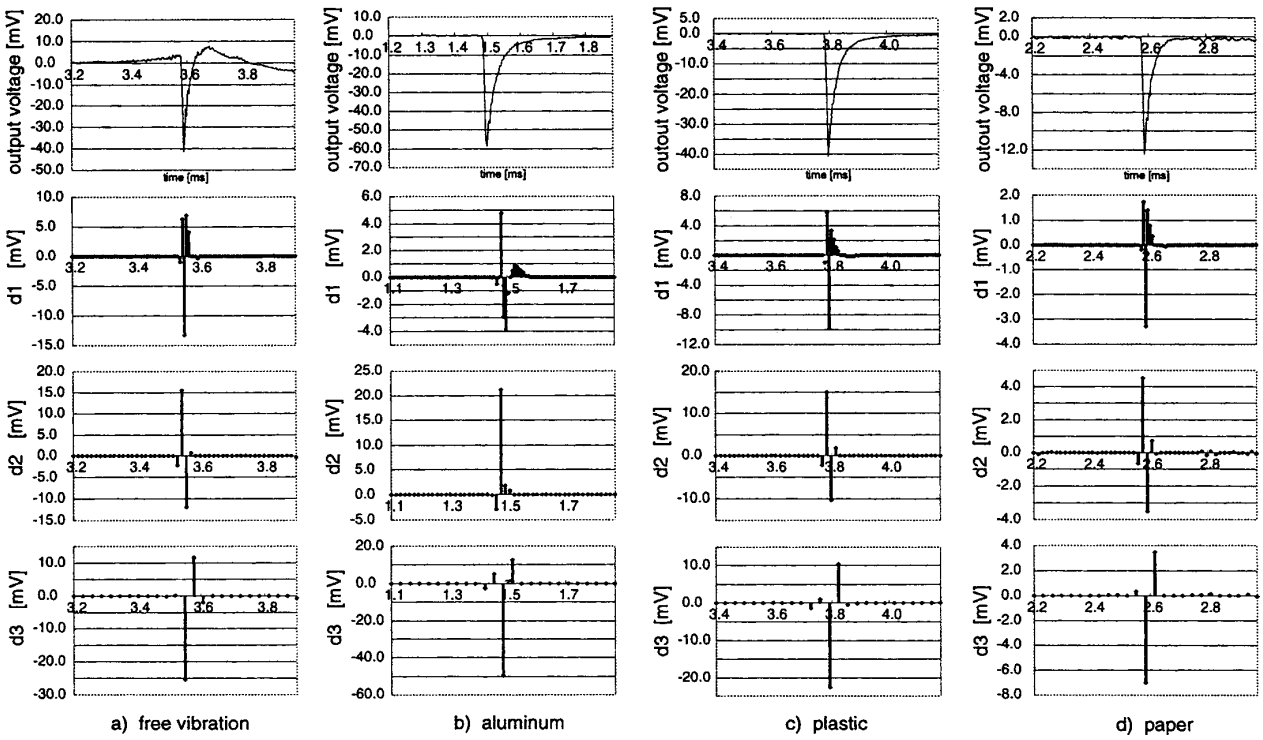


Fig. 5. Discrete Wavelet Transform of the slip signals for the three kinds of objects using Symlet(N=8) basis.

the sensor ridges, and that the impulsive signals are distinctive in the sense that they do not depend on the contact surface conditions.

4. EXPERIMENT FOR VERIFYING THE CAPABILITY OF ISOLATING A SLIP PHASE

We conducted the second experiment of observing the sensor output signals in simple yet practical manipulation of an object: the robot hand allowed the sensor surface to make contact with, roll or slip on, and break contact with an object. A two-fingered planar robot hand illustrated in Figure 6 was used as the main experimental set up.

A parallel link mechanism and a Dulon's circular motion mechanism were integrated in each of the fingers to constitute 3 degrees of freedom in their planar motion *i.e.* translational motion in the X, Y-axes, and rotational motion with respect to the Z-axis. Each finger was driven by 3 direct drive motors fixed at the base of the setup, and was either position- or force-controlled.

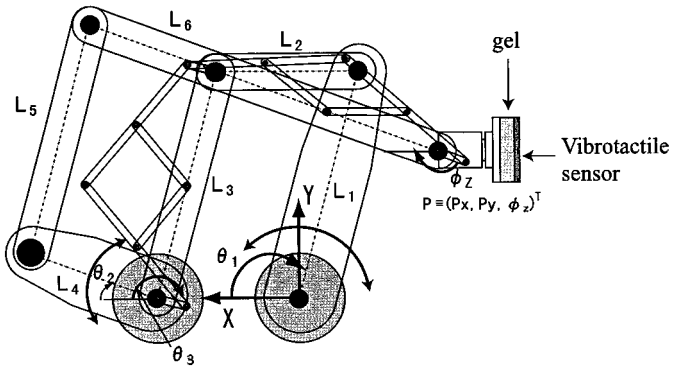


Fig. 6. Planar 3DOF finger with the sensor attached to the compliant endtip.

In the position-control mode, infinitesimal displacement of the position and orientation of the endtip $d\boldsymbol{P} \equiv (dP_X, dP_Y, d\phi_Z)^T$ was computed according to the following formula where $d\boldsymbol{\Theta} \equiv (d\theta_1, d\theta_2, d\theta_3)^T$,

$$d\boldsymbol{P} = \boldsymbol{J} \cdot d\boldsymbol{\theta}$$

and where

$$\mathbf{J} = \begin{bmatrix} -(L_1 - L_3 + L_5)\sin\theta_1 & -(L_4 - L_6)\sin\theta_7 & 0 \\ (L_1 - L_3 + L_5)\cos\theta_1 & (L_4 - L_6)\cos\theta_7 & 0 \\ 0 & 0 & 1 \end{bmatrix}$$

On the other hand, the reference torque $\boldsymbol{\tau} \equiv (\tau_1, \tau_7, \tau_8)^T$ in the force-control mode was computed from the force $\boldsymbol{f} \equiv (f_x, f_y, m_z)$ which is to be exerted at the endtip $\boldsymbol{P}$.

$$\boldsymbol{\tau} = \boldsymbol{J}^T \boldsymbol{f}$$

4.1. Sensor output by contact phase

Figure 7 shows a typical sample signal of the sensor output obtained when the surface makes contact with an aluminum

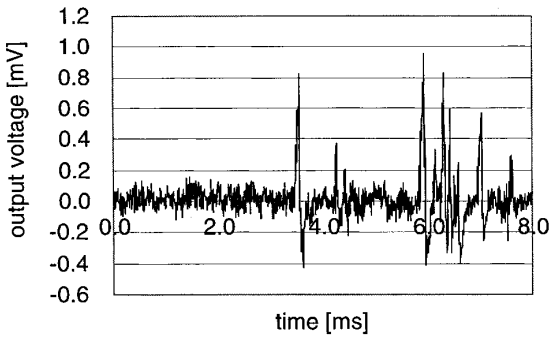


Fig. 7. Sample signal of the sensor output obtained when the sensor surface makes contact with an aluminum block.

https://doi.org/10.1017/S0263574799002453 Published online by Cambridge University Press

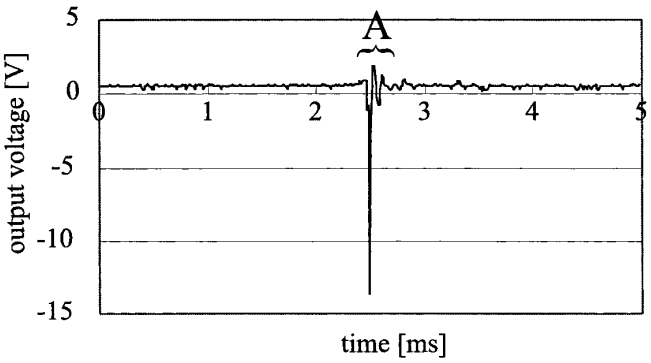


Fig. 8. Sample signal of the sensor output obtained when the sensor surface breaks contact with an aluminum block.

block. The waveform totally differs from those of slip signals in Figure 3 in that the amplitude of the impulsive signal in Figure 7 is much smaller than that in Figure 3, and we can easily neglect the phase in which the fingertip makes contact with an object.

On the other hand, Figure 8 shows another typical sample of the sensor output obtained when the robot hand breaks contact with an object. The signal in the figure resembles that in the free vibration mode of the sensor element previously shown in Figure 3. However, the impulsive signal is followed by the overshoot labeled A. Such an overshoot does not appear in any slip phase because the signal in the slip phase is generated when the deformed sensor ridge is released while it keeps contact with the object. More detailed tribological consideration suggests that the element enters the stick phase as soon as it is released from the slip phase. We define it as *release-phase overshoot*, and use this index for isolating the phases where an object is released from the sensor surface.

Furthermore, it is also required that a roll phase in object manipulation be distinguished from a slip phase. Figure 9 shows the sensor output when an aluminum cylinder is rolled on one of the sensor surface. In this experiment, the position-control mode was used for the experiment and the geometrical θ_8 data showing the roll of the fingertip in correspondence with the rolling object is also traced in the figure. As the sensor output signal associates us with the result in Figure 8, the release-phase overshoot indicated as part B is again observed in the signal. The resultant phenomenon indicates that the sensor element is released

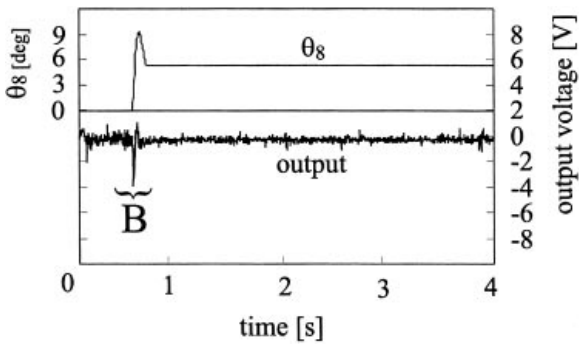


Fig. 9. Sample signal of the sensor output obtained when an aluminum cylinder rolls on the sensor surface.

into free vibration even in a roll phase. Consequently, the proposed sensor is capable of masking out the roll phase.

5. APPLICATION OF THE SENSOR TO OBJECT REGRIP CONTROL

5.1. Limitation of a slip prediction approach in flat contact cases

As was mentioned in Section 1.1, slip prediction using incipient slip information is useful for real-time grasp force control of a robot hand to prevent an object from falling. It is useful if such a distinctive interval from the onset of incipient slip to the beginning of a complete slip is expected in the case where the surface of the sensor is not flat but curved because in the curved surface case, there is some difference of normal contact force component in the contact area which enables a peripheral slip sensor element to generate slip signals more easily and earlier in translational slipping of an object. However, there is a limitation to this slip prediction approach in the case where an object makes flat contact with the sensor surface as we verified in Figure 10. In the figure, we can observe only 1*ms* difference of the onset of slip among the three signal channels of the sensor elements which are arranged as described in Section 2.

5.2. Object regrip control after isolating a slip phase

Now, we are ready for the experiment of applying one out of the three sensor signal channels to the grasp force control of the robot hand. In the experiment, the fingers initially grasp a notebook in the form of sensor-pad opposition at a grasp force f_x = 2.0*N*. After an initial state of grasping (holding) an object, the reference torque input is gradually decreased until the fingers release the object. As soon as the system identifies that the object is falling, the grasp force is instantly increased. Figure 11 shows the sensor output signal and correspondingly increased torque input during four repetitive phases of releasing and regripping the object in 2 *s*. During this interval, the notebook fell approximately 4 mm.

A closer observation of interval C in Figure 11 makes it easy to understand that the system required a time interval of 11*ms* after detecting the slip phase and before increasing

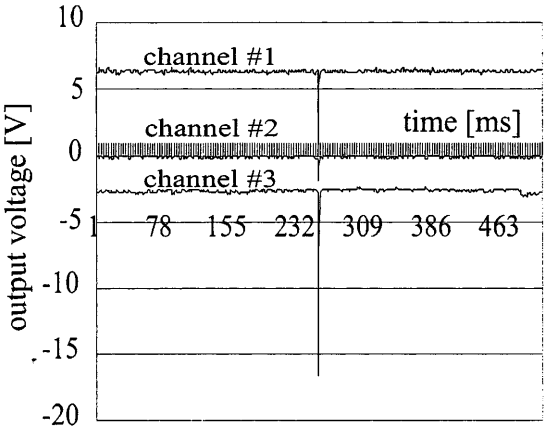


Fig. 10. Output signals of the three sensor elements. There is little difference of starting slipping instant.

https://doi.org/10.1017/S0263574799002453 Published online by Cambridge University Press

the grasp force (Figure 12). During the last 6*ms* of the above time interval, the system checks whether or not the release phase overshoot index follows the slip signal from 1.295*s* to 1.301*s*. Because there was no such index, the grasp force was increased. Note that the sharply rising signal accompanied the increase of the grasp force, which is reasonable when it is associated with the similar signal in Figure 7.

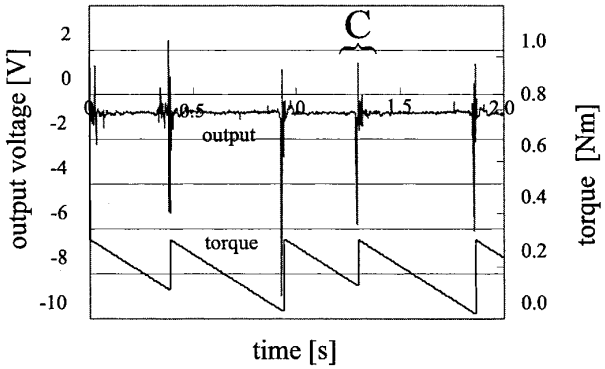


Fig. 11. Output signal and correspondingly increased torque input during four repetitive phases of the object's release and regrip.

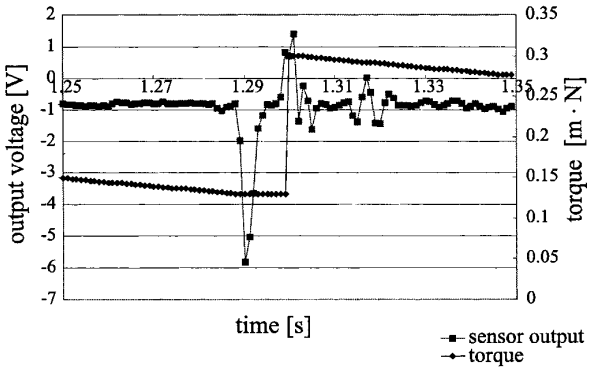


Fig. 12. Close observation of interval C in Figure 11.

Figure 13 is a sequence of four photographs demonstrating the real-time regrip control for arresting the fall of the notebook. The experiment of real-time regrip control triggered by not an incipient but a complete slip signal was successful because the frequency of the slip signal is in the order of one kilohertz. These two figures demonstrate the effectiveness of the proposed vibrotactile sensor which generates impulsive high-frequency slip signals and is capable of masking out the contact phases other than a slip phase.

6. CONCLUSION

In the study, we proposed a vibrotactile sensor with a surface-ridge structure which generates impulsive high-frequency signals and is capable of isolating slip phases from other contact phases. We then demonstrated real-time readjustment control not to drop an object using the pure-slip sensor information. The folllowing five items summarize this paper.

(i) We proposed the sensor structure with surface ridges in which PVDF film strips are vertically sandwitched in the center.

(ii) Output signals of the sensor were observed and classified into stick-slip and high-frequency vibration components. We verified that the high-frequency vibration component does not depend on the contact surface conditions while the stick-slip vibration depends on them.

(iii) A wavelet transform technique was used to analyze the impulsive slip signals when aluminum plate, a plastic plate, or a paper sheet was slid on the sensor surface. From the analysis, we can say that the slip signals exhibit a good coherence with the signal in a free vibration mode.

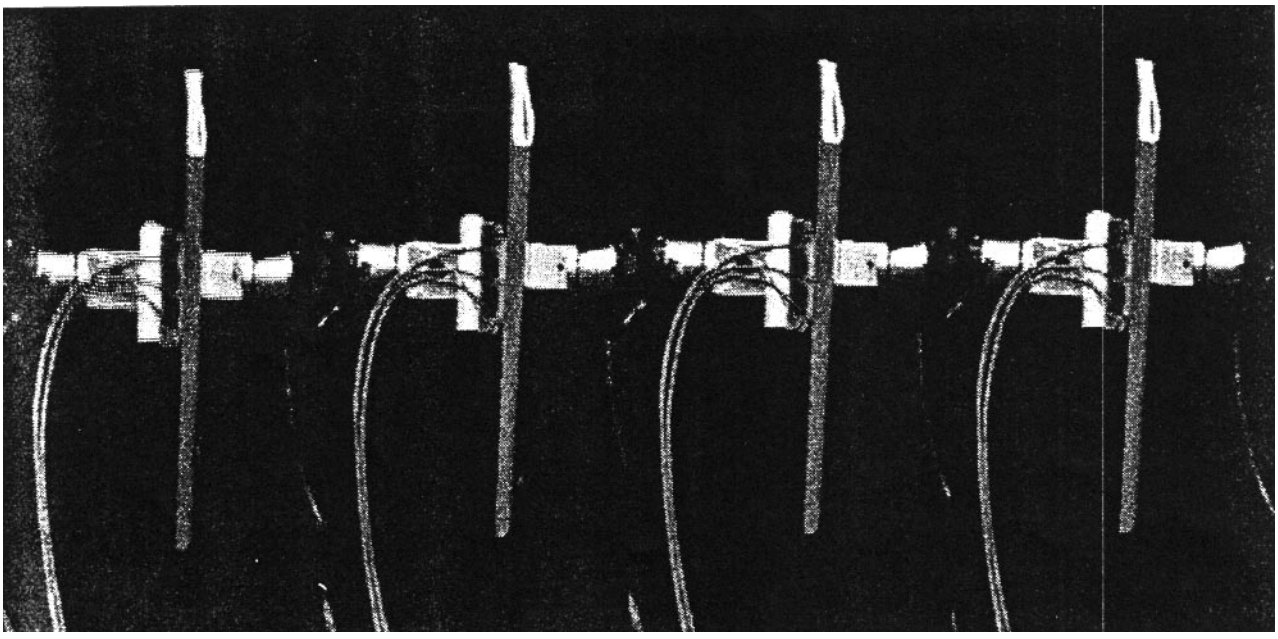


Fig. 13. Sequences of photographs of demonstrating the real-time object regrip control. The notebook slips down only 1 mm on average in a control cycle.

https://doi.org/10.1017/S0263574799002453 Published online by Cambridge University Press

(iv) The experiment using a two-fingered robot hand with the sensor attached at the endtip verified that the sensor is capable of isolating slip phases from contact, release, or rolling phases. We defined the characteristic waveform in the slip signal as released phase overshoot for neglecting release phases.

(v) The advantage of the impulsive high-frequency signal enabled the sensor system to mask out the contact phases other than a slip phase in the order of miliseconds. The effectiveness of the proposed sensor was demonstrated by real-time object regrip control for arresting the fall of a notebook.

As future work, we should continue to verify that the proposed sensor is confirmed to isolate slip phases in various and practical manipulation tasks, which requires dextrous control of the robot hand in combination with much close observation of the signals in multiple channels of the sensor.

ACKNOWLEDGEMENT

This research was partly supported by the Ministry of Education, Science, and Culture under Grant-in-Aid for Scientific Research No. 10450161.

References

1. M. Ueda and K. Iwata, "Tactile Sensor for Industrial Robot to Detect A Slip", *Proceedings of 2nd Int. Symp. on Industrial Robots* (1972) pp. 63–76.
2. R.D. Howe and M.R. Cutkosky, "Sensing skin acceleration for texture and slip perception", *Proceedings of 1989 Int. Conf. on Robotics and Automat.* (1989) pp. 145–150.
3. A. Bicchi, J.K. Salisbury and P. Dario, "Augmentation of grasp robustness using intrinsic tactile sensing", *Proceedings of 1989 Int. Conf. on Robotics and Automation* (1989) pp. 302–307.
4. M. Tremblay and Cutkosky, "Estimating Friction Using Incipient Slip Sensing During manipulation Tasks", *Proceedings of 1993 Int. Conf. on Robotics and Automation* (1993) pp. 429–434.
5. Y. Yamada, K. Santa, N. Tsuchida and K. Imai, "Active Sensing of Static Friction Coefficient", *Proceedings of 1993 Int. Conf. on Advanced Robotics* (1993) pp. 185–191.
6. B. Eberman and J.K. Salisbury Jr.,. "Application of Change Detection to Dynamic Contact Sensing", *MIT AI-memo No. 1421* (1993).
7. J.S. Son, A. Monteverde and R.D. Howe, "A Tactile Sensor for Localizing Transient Events in Manipulation", *Proceedings of 1994 Int. Conf. on Robotics and Automation* (1994) pp. 471–476.
8. M. Tremblay *et al*., "Utilising Sensed Incipient Slip Signals for Grasp Force Control", *Proceedings of 1992 Japan-USA Symp. on Flexible Autom.* (1992) pp. 1237–1243.
9. Y. Fukahori and H. Yamazaki, "Mechanism of rubber abrasion. Part I: Abrasion pattern formation in natural rubber vulcanite", *Wear* **171**, 195–202 (1994).
10. Y. Yamada *et al.*, "Vibrotactile Sensor Generating Impulsive Signals for Distinguishing Only Slipping States", *Proceedings of 1999 Int. Conf. on Intelligent Robots and Systems* (1999) pp. 844–850.
11. P. Dario, C. Domenici, R. Bardelli, D. De. Rossi and P.C. Pinotti, "Piezoelectric Polymers: New Sensor Materials for Robotic Applications", *Proceedings of 13th Int. Symp. of Industrial Robots and ROBOTS* (1983) Vol. 2, pp. 14–34–49.
12. R.D. Howe and M.R. Cutkosky, "Dynamic Tactile Sensing: Perception of Fine Surface Features with Stress Rate Sensing", *IEEE Trans. on Robotics and Automation* **9**, No. 2, 140–151 (1993).

https://doi.org/10.1017/S0263574799002453 Published online by Cambridge University Press